INSULATION DESIGN OF LOW VOLTAGE ELECTRICAL MOTORS FED BY PWM INVERTERS

L. Lusuardi and A. Cavallini
University of Bologna, 40136 Bologna, Italy

M. Gómez de la calle, J.M. Martínez Tarifa, G. Robles
Department of Electrical Engineering, Universidad Carlos III de Madrid

Key Words: inverter-fed machine, partial discharges, insulation design.

This paper proposes a model to determine the partial discharge inception voltage of magnet wires, including the effect of elevated temperatures, and shows its applicability to the complete range of wire geometries considered in IEC Standard 60317-13.

Introduction

For long, the insulation of magnet wires used in low voltage motors was mostly stressed by temperature and vibrations. Moisture helped thermo-mechanical stress by hydrolyzing the insulation easing crack formation. The ultimate breakdown mechanism was an excessive leakage current throughout cracks and pinholes in the insulation [1] [2]. Within this framework, the thickness of the insulation was dictated mostly by mechanical considerations, to prevent crack formation during manufacturing and operation. Electrical stress did not play a key role in the aging process.

Power electronics changed this picture. The highest voltage at the motor terminals due to surge reflections and the uneven turn distribution during switch commutations have raised the electrical stress levels, particularly in the turn/turn insulation [3] [4] [5] [6]. As a result, there is a concrete risk that the electrical stress exceeds the inception field for the ignition of partial discharge (PD). If PD are incepted, their number per second is often comparable to two times the carrier frequency of the inverter. For organic insulation such as the used for enameled wires, PD attack is a too-heavy duty: failure occurs within a brief time and the reliability of the insulation cannot be guaranteed [7].

To prevent PD-induced failures, the standard IEC 60034-18-41 [8] requires that an electrical insulation system (EIS) suitable for inverter duty should be PD-free long enough to ensure its reliability. To do so, one should select first a stress category, or the peak voltage of the surges expected at the motor terminals. Depending on the selected stress category, the standard defines reference test voltage levels for qualification (accelerated life tests) and type tests. Accelerated life tests (under thermo-mechanical, ambient stress) following the scheme proposed in IEC 60034-18-21 [9] are then performed. The candidate system qualifies for inverter duty if the partial discharge inception voltage (PDIV) exceeds the reference test levels (during the aging tests) longer than a reference system, i.e., a system with proven service experience.

The approach to ensure the reliability of the candidate EIS is (a) to design and manufacture it PD-free below the reference stress levels, and (b) to make sure that the combined TEAM stress factors to

not reduce the PDIV too quickly. Thus, being able to predict the PDIV is important to avoid repeating costly and time-consuming qualification procedures. Also, a model able to predict the impact of temperature can help to select in a more appropriate way the temperature enhancement factor used in [8] to account for the impact of elevated temperatures during operation.

In this paper, we focus on the turn/turn insulation, which is often the weakest insulation subsystem for inverter-fed motors. The results of PDIV tests carried out on twisted pairs (turn/turn insulation models) at 50 Hz using sinusoidal voltages on nine magnet wires having different diameter and insulation thickness are reported first. The IEC [8] allows the use of either sinusoidal or impulse voltages for twisted-pair samples but the values of the PDIV are lower for sinusoidal sources if the rise times of the impulses are below 1μs [10]; thus, the tests done at 50 Hz give a conservative assessment of the PDIV for these samples. The wires were tested at both ambient temperature and 150 °C to consider the influence of temperature on PDIV. The experimental results are first processed using multivariate regression to find out the most important parameters to design the turn/turn insulation. They also constitute a reference database used to set up a finite element method (FEM) model to predict the PDIV. The proposed model is based on the Schumann's streamer inception criterion [11], if streamer discharges are responsible for dielectric degradation rather than Townsend discharges. After showing that the model can predict the impact of elevated temperatures, the model is used extensively to infer the sensitivity of PDIV to magnet wire geometry and permittivity and to produce charts reporting PDIV values for standardized magnet wires geometries. The impact of aging on insulation thickness and PDIV [12], is not considered here.

Test samples and setup

a. Test samples

The turn/turn insulation consists of insulating varnishes deposited on the conductor in multiple passes. Polyester and polyamide-imide are the most popular dielectrics. Since the latter is costlier but ensures better resistance to abrasion and hydrolysis at elevated temperatures, polyester is often used in the inner layer (where it also provides a very good mechanical fitting with the conductor, since its yield limit and tensile strength are like those of copper). Polyamide-imide is thus used as an overcoat.

In many applications, a resin/varnish fills the space within adjacent conductors to bond the wires together and to the stator, ensure better thermal exchange properties and environmental protection. The selection of the insulator/varnish pair is sometimes an issue due to incompatibility, and is based on experience: with time, the resin should not detach from the conductors exposing pinholes and leaving free space where PD could be incepted. Indeed, for a conservative electrical design, the resin could be considered only as a mean to improve thermal exchange, mechanical stability, and ambient protection. Thus, one can assume that voids could exist within the insulation due to an incorrect impregnation (e.g., varnish leaking out of the stator due to a curing procedure insufficient to ensure gelification of the varnish). Indeed, it was reported that even turn to turn insulation of VPI machines can suffer PD activity when subjected to steep-fronted voltage pulses [13]. For this reason, reference will be made in this paper to twisted pairs that, on purpose, were not immersed in resin.

Table I - Properties of the twisted pairs.

	Code	D_{out} (mm)	Thick. (μm)	ε_r @25 °C	ε_r @120 °C
1	W1	0.40	16	4.53	4.24
2	W2	0.60	18	3.87	4.15
3	W3	0.80	24	3.74	3.89

4	W4	0.62	29	4.55	4.59
5	W5	0.59	30	3.99	3.73
6	W6	1.00	30	4.09	4.20
7	W7	1.71	40	3.14	3.53
8	W8	1.20	42	3.60	3.61
9	W9	1.80	43	3.56	3.52

Twisted pairs were realized using nine different magnet wires. An effort was made to characterize as fully as possible the enamel thickness and properties of these wires. The collected data are summarized in Table I.

The external diameter of the wire D_{out} (used to obtain the enamel thickness) was measured using a micrometer with a 1 μm scale division. For each kind of wire, a measurement was taken every 20 cm up to a total of five. After removing the insulation by a chemical process that does not erode the copper surface [14], the same was done for the diameter of the bare conductor D_{in}. The values for the enamel thickness, t, are obtained according to:

$$t = \frac{D_{out} - D_{in}}{2} \qquad (1)$$

The diameter of the cable and the enamel thickness fit the relationship established by the IEC Std. IEC60317-13 [15] for grade 2 conductors, as Fig. 1 shows. Note that, as prescribed in [14], the enamel thickness increases with the diameter of the cable.

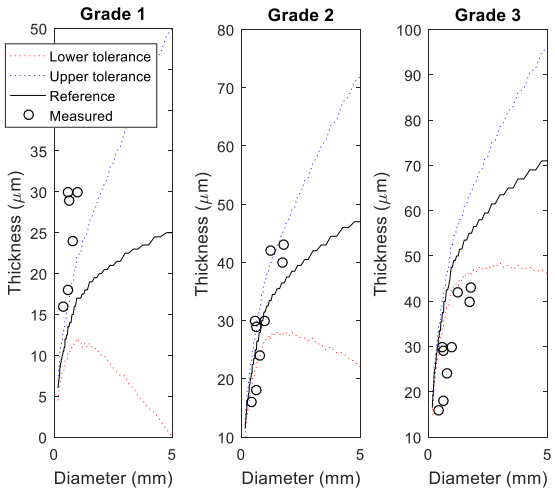

Fig. 1. Scatterplots representing the insulation thickness versus the conductor diameter. The plots also show the reference insulation thickness and its tolerance as a function of conductor diameter for the three grades of insulation established in [15]

To estimate the permittivity of the insulation, a High-Resolution Dielectric Analyzer (Novocontrol Technologies Alpha-N) measured the insulation coating of a 10 cm wire section at 50 Hz. The use of this frequency is appropriate for this work since the experimental measurements have also been made at 50 Hz. For many applications using square wave voltages, we expect little difference between the permittivity measured at 50 Hz and that necessary to model the electrical field harmonics, since the frequency content is probably lower than the limits of dipolar polarization. Indeed, further investigations at higher frequencies might become necessary when wide bandgap devices having an extremely large slew rate are employed. For this purpose, the insulation coating of the wire was

removed at one end, while the middle part was painted with conductive paint to create the ground electrode. The values for the capacitance were then used to determine the real part of the permittivity ε_r according to:

$$\varepsilon_r = \frac{C_p \ln(D_{out}/D_{in})}{2\pi\varepsilon_0 l} \qquad (2)$$

where C_p is the measured capacitance, ε_0 is the vacuum permittivity and l is the length of the wire.

Figure 2 shows the permittivity values based on the average value recorded over 10 samples for each wire, both at room temperature and at 120°C. In the latter case, the samples were put in an oven. Fig. 2 shows the results obtained as a function of the insulation thickness. As can be seen in this figure and Table I, at higher temperatures, the permittivity tends to be lower, with a mean reduction of 9.7%. For the dielectric with the lowest permittivity, the reduction is more marked (25%).

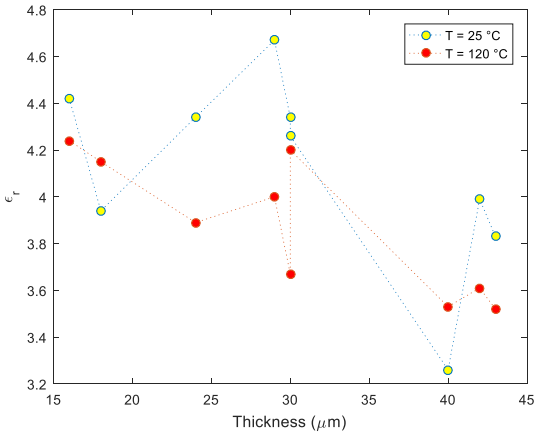

Fig. 2. Insulation thickness versus the relative permittivity of the insulation at 25 °C and 120 °C based on experimental results.

b. Test setup

The circuit detailed in Fig. 3 is used to measure PD activity in twisted pairs. It is a standard indirect detection circuit [16] which measures conducted current pulses through a capacitive mesh. One of the terminals of the twisted pair is connected to the high voltage output of the source, while the other one to the ground. The generator is a variable sinusoidal voltage source (GLP1-e HV by Schleich). The advantage of using this voltage source is the 'ramp' function, which allows controlling the applied root mean square (RMS) voltage. The voltage source is programmed using a ramp time of 240 s and a maximum voltage of 1200 Vrms. After an initial period, the voltage is increased in steps of 25 V. Using this configuration data, each voltage step is maintained for 6 s, which has proven to be enough to detect PD activity. Once a repetitive PD activity is detected in a commercial acquisition system, the applied voltage is disconnected and the PDIV recorded.

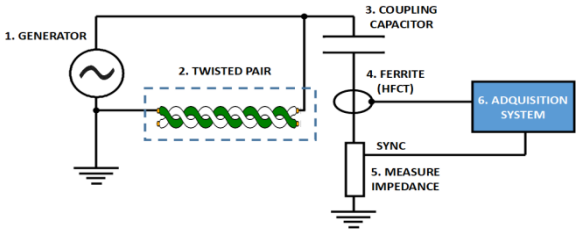

Fig. 3. Test circuit.

To get statistical reliable data, a set of ten samples per each magnet wire of 20 turns has been produced.

Statistical analysis

The data collected performing PDIV tests were modeled using the Weibull distribution and analyzed via multivariate techniques to spotlight which parameters (thickness, conductor diameter and permittivity) play a dominant role in determining the PDIV of a twisted pair sample. In fact, the permittivity of the material was not correlated with PDIV in an appreciable way, possibly due to measurement errors (capacitance measurement were performed on wires, not flat specimens), and the limited sample size.

In Table II, the 10th percentile (B_{10}), the scale and shape parameters are reported for the tests performed at 25 °C and 150 °C. The B_{10} parameter is reported to provide an estimate of what happens in the worst case, i.e., when the inception voltage is close to its statistical minimum.

Table II – PDIV values obtained during the experiments (n=10).

		PDIV @25 °C			PDIV @150 °C		
	Code	B_{10} (V_{pk})	α (V_{pk})	β	B_{10} (V_{pk})	α (V_{pk})	β
1	W1	567	596	44.66	512	519	188.1
2	W2	578	582	302.2	577	580	333.8
3	W3	623	686	23.23	588	645	24.14
4	W4	693	725	50.19	625	650	56.61
5	W5	734	767	50.89	701	706	335.7
6	W6	756	813	31.22	636	683	31.47
7	W7	854	915	32.63	758	788	57.8
8	W8	848	883	54.35	787	818	58.53
9	W9	877	925	41.84	781	820	45.65

In [14], we observed that PDIV data tend to align to a straight line when plotted versus insulation thickness, *t*. To understand whether the magnet wire diameter (D_{out}) could also be of interest, a multivariate linear function having the form:

$$B_{10} = \theta_0 + \theta_1 \cdot t + \theta_2 \cdot D_{out}^n \qquad (3)$$

was fit to the data. Indeed, changing the power *n* from 0.1 to 2 did not provide any θ_2 larger than its standard error (for instance, considering *n=1*, the p-values for D_{out} were 0.687 and 0.85 for 25 °C and 150°C) [17].

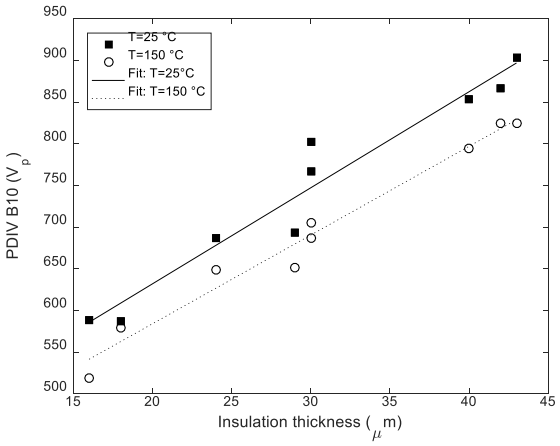

Fig. 4. Scatterplot of PDIV B10 versus insulation thickness.

Inspecting the simple univariate models obtained using the insulation thickness (see Table III) one observes that all parameters are well above the significance level. Also, the constant terms θ_0 (401 V at 25 °C, 371 V at 150 °C) are of interest in that they can be used as worst case to design an intrinsically PD-free insulation.

Table III – Linear models fitting B_{10} PDIV data as a function of insulation thickness.

Par	Estimate	Std. Err.	t value	Pr(|θ|<t)
T = 25 °C				
θ_0	401 V	29.6 V	13.5	9.9×10^{-6}
θ_1	11.5 V/μm	0.93 V/μm	12.3	17.4×10^{-6}
T = 150 °C				
θ_0	371 V	18.3 V	20.2	0.9×10^{-6}
θ_1	10.6 V/μm	0.57 V/μm	18.3	1.7×10^{-6}

FEM Model based on Schumann criterion

The Paschen curve can describe the onset of breakdown phenomena in uniform fields under quasi-static conditions. However, many phenomena of engineering importance take place in non-uniform electric fields; in this case, in addition, the electrodes are covered by an insulation film. In these conditions, the Paschen curve has no validity since the emission of secondary electrons from the insulated cathode by positive ion or UV bombardment is extremely unlikely (the work function of e.g. copper is 4-5 eV, whereas in an insulator is 9 eV [18]). Therefore, it cannot be used to predict the breakdown voltage and must be replaced by the streamer inception criterion.

The main feature of the streamer concept is the single-electron-avalanche mechanism. It is generally assumed that breakdown occurs when the number of electrons N_e in an electron avalanche reaches a critical value N_c. In literature, this number is often considered equal to 10^8 for air, irrespective of the specific conditions under consideration [18].

The distance traveled along a field line by an avalanche before growing to the critical number of electrons is called critical length d. In a non-uniform field, such as the one currently under examination, *d* is the distance from the insulated electrode along the field line in question to the point beyond which the growth of the avalanche stops, i.e. the point at which $\alpha_{eff} = 0$ being α_{eff} the effective ionization coefficient of the anode.

The number of carriers in the head of the avalanche at a distance *x* from the point where it originated, assumed that it is started by a single initial electron [11], is:

$$N(x) = \exp\left(\int_0^x \alpha_{eff}(x')\mathrm{d}x'\right) \qquad (4)$$

where the effective ionization coefficient depends on the gas nature and on the reduced electric field E/p [18]. The relationship $\frac{\alpha_{eff}}{p} = f\left(\frac{E}{p}\right)$ for dry air is found in the LXCAT database (last update in July 2016) [19]. Thus, according to Schumann [11], the streamer inception criterion is:

$$\int_0^d \acute{\alpha}(x)dx = K \qquad (5)$$

where *K* is a dimensionless constant, generally taken as $K = 18 \approx ln(10^8)$. Contrarily to what could be expected inspecting eqns. (4) and (5), it is possible to demonstrate that [20]:

$$K \neq ln\, N_c \qquad (6)$$

Therefore, there is no reason for retaining *K* equal to 18. Pedersen suggests that the value of the constant K in (5) can be computed [21], making precise measures of sparking voltage V_s in a uniform field. Indeed, in this case, (5) is simplified as follows:

$$K = \alpha_{eff}(V_s/d)d \qquad (7)$$

According to Malik [22], when $p \cdot d$ is less than 1 bar·cm (as this is the case for air wedges in twisted pairs), the calculated values of breakdown voltages using $K = ln(10^8)$ are up to 50% higher than the measured values. Likewise, a decade later Zaengl and Petcharaks obtained $K \approx 9$ [23].

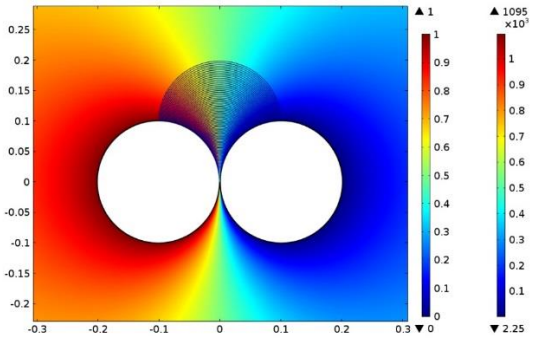

Fig. 5. Modeling of the electric field of an insulated twisted pair.

Therefore, it is necessary to have experimental measures to determine the proper value of *K* for the geometry of twisted pairs. To start with, a simplified FEM analysis of the electrical field in a twisted pair was carried out using Comsol Multiphysics®. The model is composed of two circular conductors, separated and enclosed by an insulating layer of enamel, see Fig. 5. Electrostatic simulations for wires having different diameter and insulation thickness were performed initially with a unitary voltage, to obtain a reference database. For a specific type of wire, simulations were carried out as follows:

1. Set V=PDIV (peak value);

2. Determine the electrical field across each field line in the air wedge between the wires;
3. Import the database of gas ionization parameters as a function of the specific electric field $\acute{\alpha}(E/p)$;
4. Start from *K=18*;
5. Evaluate left term of eqn. (5) for each electric field line;
6. If $\int_0^d \alpha_{eff}(x)dx \geq K$ for at least one electric field line STOP, otherwise reduce K and start again from #5.

When condition 6 is met, the shortest field line satisfying eqn. (5) is taken as the discharge line. Table IV shows the value of *K* which satisfies eq. (5) for the different twisted pairs used and the associated products $p \cdot d$ (the pressure is always quite close to 1 bar). To determine the PDIV for any arbitrary case, the average value K=5.98 was considered.

Table IV - Experimental evaluation of the Schumann constant.

Code	$p \cdot d$ (bar cm)	K
W1	0.0018	5.79
W2	0.0032	5.36
W3	0.0031	5.30
W4	0.0037	6.08
W5	0.0038	6.26
W6	0.0039	6.58
W7	0.0036	5.94
W8	0.0037	6.12
W9	0.0041	6.42
Average	0.0034	5.98

To account for different temperatures, the model is used with an equivalent pressure. The equivalent pressure is derived by considering the air around the wires as a perfect gas (which is true for a wide range of pressure and temperature values typical of engineering applications), thus following the law:

$$p = nk_BT \quad (8)$$

Where k_B is the Boltzmann constant, *n* the number of gas molecules per unit volume, *p* and *T* the gas pressure and temperature, respectively. At a given altitude, the pressure of the air in contact with the winding is constant. Therefore, increasing the temperature from the ambient temperature, T_A to an elevated temperature T_H affects the number of gas molecules per unit volume:

$$p / k_B = n_A T_A = n_H T_H \Rightarrow n_H / n_A = T_A / T_H \quad (9)$$

The effective ionization coefficient is generally reported as a function of the reduced electric field *E/p* evaluated at ambient temperature. However, considering the physics of gas discharges, the ionization coefficient depends on the kinetic energy, *W*, acquired by an electron in a mean free path, λ. Since λ is proportional to the reciprocal of the number of molecules per unit volume:

$$W = E \cdot \lambda \propto E / n \propto E / p \quad (10)$$

Most ionization models relate changes in air density with changes in pressure, but during motor operation, pressure is constant (around 1 bar), and it is the temperature the variable which influences

the air density. To model this situation, considering the last two terms in eqn. (10), one can define an equivalent pressure p_H^* that, at ambient temperature, will provide the same number of gas molecules per unit volume observed at T_H. Thus, one can write:

$$\frac{E/p_A}{E/p_H^*} = \frac{E/n_A}{E/n_H} \Rightarrow p_H^* = p_A \frac{n_H}{n_A} \qquad (11)$$

Combining eqns. (9) and (11) one finally achieves the equivalent pressure to be used in the simulations at elevated temperatures:

$$p_H^* = p_A (T_A / T_H) \qquad (12)$$

Once all parameters are defined, the following iterative approach is used to determine the PDIV for a given configuration:

1. Set the initial voltage equal to 100 V in the 2D electrode system shown in Figure 5 and evaluate the electric field.
2. Import the database of gas ionization parameters as a function of the specific electric field $\alpha_{eff}(E/p_H^*)$.
3. *Set K=5.98* as explained before.
4. Verify if (5) is satisfied for at least one field line. If this does not happen, repeat from step 2 increasing the applied voltage.

Model accuracy

To show the accuracy of the proposed approach, the fitting errors for PDIV measurements performed at 25 °C and 150 °C were evaluated. Comparing the model results with experimental data at room temperature (25 °C) shows the capability of the model to fit the data. Using the same model at 150 °C serves the purpose of evaluating its extrapolation capability and has a much larger relevance to confirm the model validity.

The results of measurements and simulations are summarized in both Table V as well as in Figures 6 and 7. It can be noted that the maximum relative error is 9 % at both 25 °C and 150 °C. The voltage difference is within the voltage step range used for the ramp during the measurements of PDIV. This result support the accuracy of the model for both fitting and extrapolation of PDIV data. Therefore, we shall examine next the effect of magnet wire geometry and permittivity throughout the range of geometries defined in the IEC Std. 60317-13.

Table V – Comparison between experimental and theoretical (K=5.98) data.

Wire Code	Air temperature			
	25 °C		150 °C	
	$PDIV_{th}$ (V_{pk})	ΔV (V_{pk})	$PDIV_{th}$ (V_{pk})	ΔV (V_{pk})
W1	580	13	536	24
W2	628	50	556	-21
W3	678	56	611	23
W4	685	-8	621	-4
W5	711	-23	651	-50
W6	707	-49	639	3
W7	859	5	721	-37
W8	834	-14	727	-60
W9	841	-36	739	-42

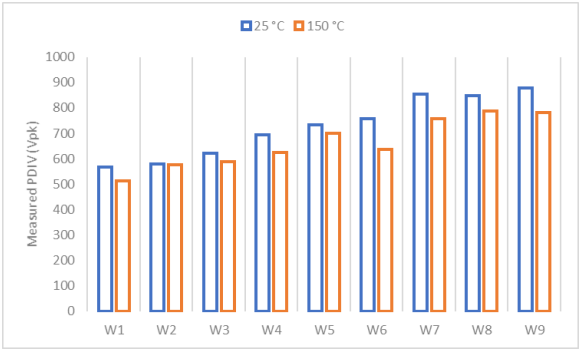

Fig. 6. Results of the PDIV measurements.

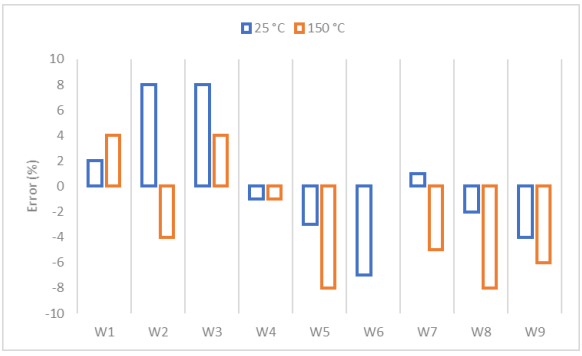

Fig. 7. Comparison between experimental and theoretical (K=5.98) data.

Dependence of PDIV on magnet wire parameters

PDIV depends almost linearly on insulation thickness, as emphasized by Fig. 4 The thickness of the enamel is the single most important parameter to determine the PDIV, a fact that is known since long [4]. According to the statistical analysis reported previously, the slope of the line is 11.5 V/μm at room temperature. At 150 °C, the slope seems to be somehow lower, 10.6 V/μm, but this is probably related to the low sample size used to perform the PDIV measurements. In fact, the difference is below the standard errors shown in Table III.

The effect of the conductor diameter has been considered rarely. Here, it was estimated for all diameters considered in the IEC Std. 60317-13 for a few insulation thicknesses and two representative values of permittivity (ε_r=3.5 and 4.5). Fig. 8 shows the result of the simulation highlighting that larger diameters exhibit lower PDIV values. This figure represents relative PDIV values: simulated PDIV compared to a base value for each insulation thickness.

The largest variations are observed for conductor diameters below 1 mm and, specially, for larger thickness levels. For diameters above 0.5 mm, the dependence on the diameter is not marked and can be neglected as a first approximation. Considering the range of wire diameters (≥0.4 mm) and insulation thicknesses (≤43 μm) used to derive the model (see Table I), and considering these results, it is not surprising that the effect of the conductor diameter was not statistically significant.

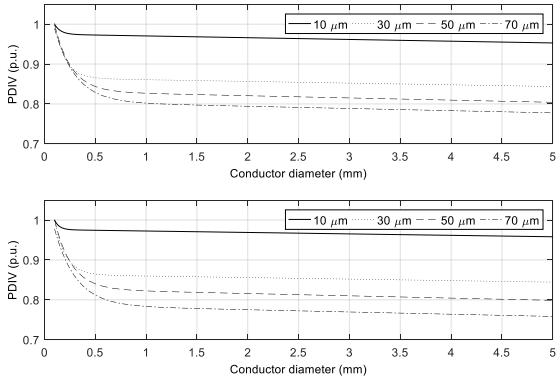

Fig. 8. Dependence of PDIV on conductor diameter for different insulation thickness and permittivity. Relative permittivity: (top) ε_r=3.5, (bottom) ε_r=4.5. Base values for increasing thickness: (top) 561 V, 863 V, 1106 V and 1351 V; (bottom) 531 V, 802 V, 1008 V and 1232 V.

Next, we investigated the impact of permittivity. One can expect that lower permittivity values provide higher PDIV values, since the mismatch between gas and solid permittivity is lower (indeed, Sumitomo attempted to manufacture a "foamed" magnet wire to reduce the solid insulation permittivity, thus raising the PDIV [24]). As a matter of fact, Fig. 9 confirms this intuitive result. Besides, Fig. 9 provides a quantitative insight on the impact of permittivity on PDIV showing that, in the worst case (assumed permittivity 2.5, actual permittivity 4.5), the reduction of the PDIV can be larger than 20%.

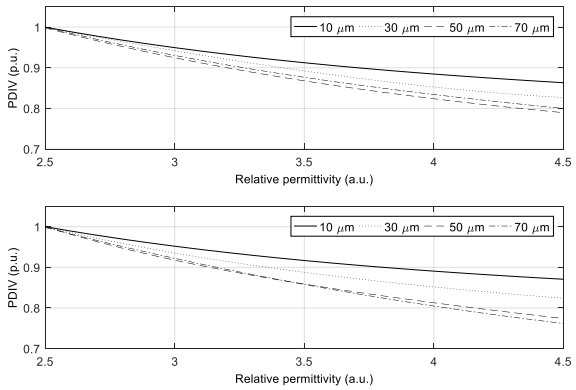

Fig. 9. PDIV as a function of solid dielectric permittivity. Conductor diameter: (top) D=0.2 mm, (bottom) D=2 mm. Base values for increasing thickness: (top) 615 V, 971 V, 1276 V and 1541 V; (bottom) 589 V, 830 V, 1055 V and 1238 V.

Eventually, the effect of temperature is investigated up to 200 °C. It is worthwhile to underline that, in doing this, it is tacitly assumed that the ionization coefficient does not vary appreciably with temperature (an assumption which was confirmed by solving the Boltzmann equations through the software Bolsig [25]). This implies that the changes in PDIV can be traced back only to the different number of gas molecules per unit volume and can be accounted for by the procedure described above. Indeed, considering the dependence of the electrical field on permittivity and the fact that, within the limits set forth by the insulation operating temperatures, increasing the temperature leads to a reduction of dipolar polarization in enamels (thus, permittivity) the results obtained through this procedure are probably a conservative estimate of the PDIV behavior . A more accurate analysis would entail measuring the dependence of permittivity on temperature up to the maximum operating temperature of the motor.

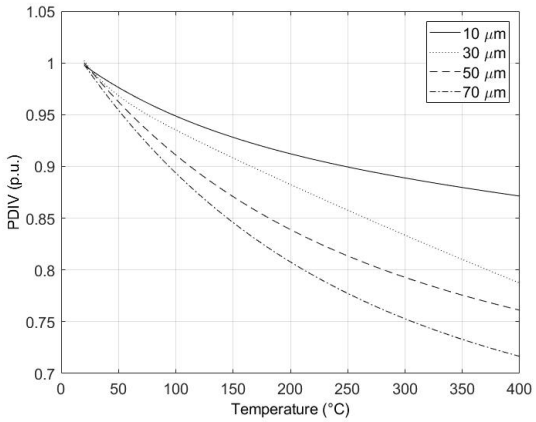

Fig. 10. Dependence of PDIV on temperature. Diameter 1 mm, ε_r=4.
Base values for increasing thickness: 526 V, 711 V, 867 V and 1023 V for 10, 30, 50 and 70 μm respectively.

To provide data that could be readily employed for industrial applications, we applied the model to the insulation diameters and thicknesses standardized by the IEC Std. 60317-13. We derived the minimum and maximum insulation thickness for each diameter and grade, thus evaluating the minimum and maximum PDIV at a given temperature, diameter and wire grade. Calculations were carried out for ε_r=3.5 and ε_r=4.5 and are shown in Fig. 11 and Fig. 12 using shaded areas. Overlapping regions can be observed since the colors are partially transparent.

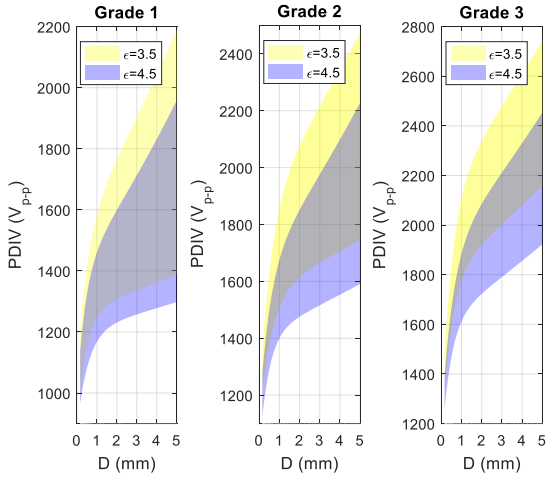

Fig. 11. PDIV ranges for the wires defined in the IEC Std. 60317-13. Temperature = 25 °C.

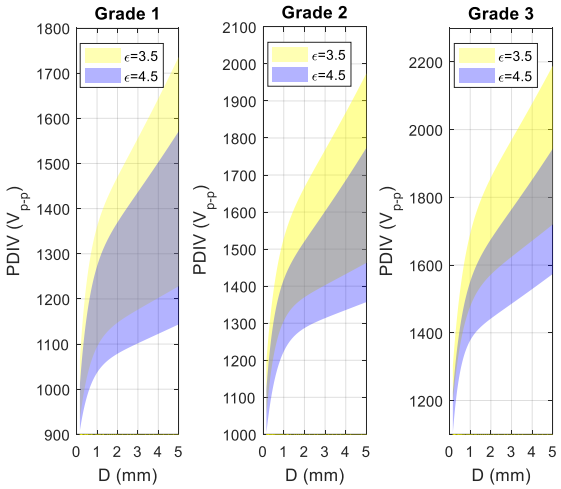

Fig. 12. PDIV ranges for the wires defined in the IEC Std. 60317-13. Temperature = 200 °C.

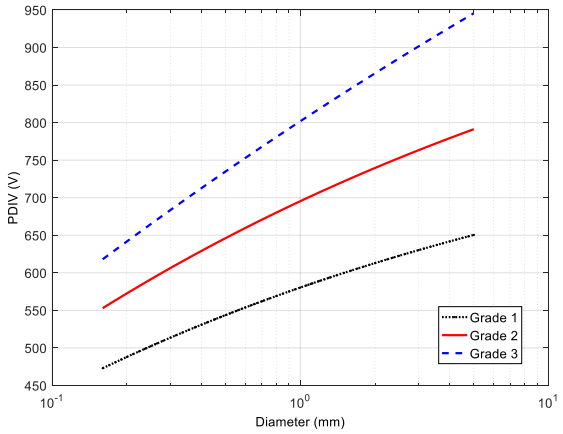

Fig. 13. Worst case curves at ambient temperature (εr=4)

Eventually, as a tool for motor design, Fig. 13 shows the worst case PDIV values as a function of conductor diameter (if the thickness is the minimum one stipulated in [15]). Based on the diameter of the wires, one can readily inspect the chart to estimate the worst case PDIV. Based on this analysis, one can decide how critical is the impregnation of the motor to achieve a sufficient reliability. Alternatively, for grade 1 and 2 magnet wires, a decision can be made to change the grade of the magnet wire.

Conclusions

According to the data reported here, the most sensitive parameter to determine the PDIV is the insulation thickness. Using multivariate models, the radius of the conductor did not provide any significant contribution in improving the estimate accuracy and can be neglected for wires having diameter larger than 0.4 mm. The permittivity of the insulation has an impact on PDIV, but considering the limited range of permittivity values in magnet wires, its sensitivity is not as large as that of the insulation thickness. In practice, to build a suitable PDIV model, estimation of the permittivity must be carried out, but its precision does not need to be extremely large.

The streamer inception criterion is a suitable tool to predict the PDIV in twisted pairs if the impregnation varnish is not considered (a conservative approach). The combined impact of pressure and temperatures can be modeled by adjusting the pressure at ambient temperature to keep the density

of the air at the correct level. The proposed model gave good prediction capability at elevated temperatures.

Using the model proposed here to predict PDIV variations induced by thermal degradation in a more accurate way is an interesting topic to work on in the future, since some results have been obtained previously about the influence of ageing on dimensions of wires [12] and an enhancement factor has been proposed in [8] to make sure that PDIV do not drops below rated voltages during operation.

The charts proposed in the last section, based on diameter/thickness relationship defined in [15] can help motor designers to achieve specified PDIV levels in a conservative approach.

References

[1] A. M. Bruning and F. J. Campbell, "Aging in wire insulation under multifactor stress," in *IEEE Trans. on Electr. Insul.*, vol. 28, no. 5, pp. 729-754, Oct 1993.

[2] P. Mancinelli, S. Stagnitta and A. Cavallini, "Qualification of Hairpin Motors Insulation for Automotive Applications," in *IEEE Transactions on Industry Applications*, vol. 53, no. 3, pp. 3110-3118, May-June 2017.

[3] E. Persson, "Transient effects in the application of PWM inverters to induction motors," *IEEE Trans. Ind. Appl.*, vol. 28, pp. 1095-1101, 1992.

[4] M. Kaufhold, G. Borner, M. Eberhardt and J. Speck, "Failure mechanism of the inter-turn insulation of low voltage electric machines fed by pulse-controlled inverters," in *IEEE Electr. Insul. Mag.*, vol. 12, no. 5, pp. 9-16, Sept.-Oct. 1996.

[5] G. C. Stone, S. Campbell, S. Tetreault, "Inverter-fed drives: Which motor stators are at risk?", *IEEE Ind. Appl. Mag.*, vol. 6, pp. 17-22, 2000.

[6] W. Yin, "Failure mechanism of winding insulation in inverter-fed motors," IEEE Electr. Insul. Mag., vol. 13, no. 6, pp. 18-23, 1997.

[7] Billard, Lebey, Fresnet; "Partial Discharge in Electric Motor Fed by a PWM Inverter: Off-line and On-line Detection"; IEEE Trans. On Dielectr Electr. Ins. Vol 21. Nº4, pp1235-1242; 2014.

[8] IEC 60034-18-41 Rotating electrical machines – Part 18-41: Partial discharge free electrical insulation systems (Type I) used in rotating electrical machines fed from voltage converters - Qualification and quality control tests, 2014.

[9] IEC 60034-18-21, *Rotating electrical machines - Part 18-21: Functional evaluation of insulation systems - Test procedures for wire-wound windings - Thermal evaluation and classification*, 2012.

[10] C. Abadie, "On-line non-intrusive partial discharge detection in aeronautical sytems", PhD dissertation, University of Toulouse, 2017.

[11] W.O. Schumann, Über das Minimum der Durchbruchfeldstärke bei Kugelelektroden, *Archiv* für Elektrotechnik, vol. 12, pp. 593-608, 1923. (in German)

[12] A. Cavallini, "Reliability of low voltage inverter-fed motors: What have we learned, perspectives, open points," 2017 International Symposium on Electrical Insulating Materials (ISEIM), Toyohashi, 2017, pp. 13-22.

[13] M. S. Moonesan, S. Jayaram, E. Cherney, R. Omranipour and S. U. Haq, "Analysis of times-to-failure of various turn insulations of form-wound coils under PWM voltage waveform," 2013 IEEE Electrical Insulation Conference (EIC), Ottawa, ON, 2013, pp. 187-190.

[14] L. Lusuardi, A. Cavallini, P. Mancinelli, G. M. De La Calle, J. M. Martinez-Tarifa, G. Robles, "Design criteria for inverter-fed Type 1 motors", in Proceedings of the IEEE International Conference on Dielectrics, 2016, pp. 605-608

[15] IEC Std. 60317-13, *Specifications for particular types of winding wires - Part 13: Polyester or polyesterimide overcoated with polyamide-imide enamelled round copper wire, class 200, 2010.*
[16] IEC 60270, *High-voltage test techniques - Partial discharge measurements*, 2000
[17] D. C. Montgomery, *Introduction to Statistical Quality Control*, John Wiley & Sons, 2008.
[18] E. Kuffel, W. S. Zaengl, and J. Kuffel, *High voltage engineering – Fundamentals*, Oxford, U.K.: Newnes, 2000.A. Fridman, *Plasma Chemistry*, Cambridge University Press, July 2008.
[19] Phelps Database from LXcat, http://www.lxcat.net/, Accessed: 2016-06-13.
[20] A. Pedersen, "On the Electrical Breakdown of Gaseous Dielectrics – An Engineering Approach", in *IEEE Trans. on Electrical Insulation*, vol. 24, no. 5, pp. 721-739, Oct. 1989.
[21] A. Pedersen, I.W. McAllister et al., "Formulation of the streamer breakdown criterion and its application to strongly electronegative gases and gas mixtures", in *Archiv für Elektrotechnik*, vol. 67, pp. 395–402, 1984.
[22] N. H. Malik, "Streamer Breakdown Criterion for Compressed Gases," in *IEEE Electr. Insul. Mag.*, vol. 16, pp. 463-467, 1981.
[23] W. S. Zaengl and K. Petcharaks, "Application of streamer breakdown criterion for inhomogeneous fields in dry air and SF_6", Gaseous dielectric VII, Ed. By L.G. Christophorou and D.R. James, Plenum press, pp. 153-160, 1994.
[24] S. Ota, M. Yamauchi, A. Mizoguchi, K. Yoshida, and Y. Tamura, "Magnet Wire with Enhanced Tolerance for High Frequency Voltage", *SEI Technical review*, no. 84, pp. 97-101, April 2017.
[25] A. Chachereau and S. Pancheshnyi, "Calculation of the effective ionization rate in air by considering electron detachment from negative ions," in *IEEE Transactions on Plasma Science*, vol. 42, no. 10, pp. 3328-3338, Oct. 2014.

Luca Lusuardi (MS'16) was born on 16 September 1991. In March 2016 he received the M.S. degree in energy and nuclear engineering from the University of Bologna (Italy), where is currently pursuing the Ph.D. degree in biomedical, electrical and systems engineering. In June 2017 he joined IEEE Dielectrics and Electrical Insulation Society. His research interests are diagnosis of insulation systems by partial discharge analysis, the study of the ageing mechanisms of rotating electrical machines and reliability of inverter-fed low voltage motors, especially in the aeronautical and automotive fields.

Andrea Cavallini (M'95) was born on 21 December 1963. He received from the University of Bologna the master's degree in electrical engineering in 1990 and the Ph.D. degree in electrical engineering in 1995. He was a researcher at Ferrara University from 1995 to 1998. Since 1998, he is an Associate Professor at Bologna University. He was cofounder of spinoff company Techimp HQ Spa. His research interests are diagnosis of insulation systems by partial discharge analysis, reliability of electrical systems and artificial intelligence. He is author or coauthor of more than 250 international papers and holds 16 international patents. He is member of IEC TC 2/MT 10.

Manuel Gómez de la Calle was born in Segovia, Spain, in 1987. He received an Industrial Engineering degree (major in Electronics) from the Universidad Pontificia de Comillas (ICAI) de Madrid, Madrid, Spain, in 2010. Since 2014, he started to pursue the Ph.D. degree in the Universidad Carlos III de Madrid, Madrid. In September 2018, he joined the Departamento de Ingeniería Eléctrica, Universidad Pontificia de Comillas (ICAI), Madrid as part-time professor for the Electrical Machines Laboratory. His research interests include the reliability of electrical systems feed by PWM inverters and partial discharge measurement at different voltage and environmental conditions.

Juan Manuel Martínez-Tarifa (M'05, SM'15) was born in Lorca, Spain in 1975. He received the M.Sc. degree in electronic engineering from the Universidad de Granada, Spain in 1999, and the M.Sc. degree in physics from the Universidad de Granada, Spain in 2000. He received the Ph.D. degree in electrical engineering from the Universidad Carlos III de Madrid, Spain in 2005. From 2000 to 2012 he was an Assistant Professor in the Department of Electrical Engineering in the Universidad Carlos III of Madrid (UC3M), where he is currently an Associate Professor. He is currently the Supervisor at the High Voltage Research and Tests Laboratory (LINEALT) at UC3M where he is working on the diagnosis of insulation systems within power cables and electrical machines. He has published over 60 articles in International Journals and Conferences. He has joined several research teams to work in over 10 research projects financed by public and private funds.

Guillermo Robles (M'02-SM'12) was born in Madrid, Spain, in 1969. He received the M.Sc. and Ph.D. degrees in electronic engineering from the Universidad Pontificia de Comillas de Madrid, Madrid, Spain, in 1993 and 2002, respectively. In 2002, he joined the Departamento de Ingeniería Eléctrica, Universidad Carlos III de Madrid, Madrid, where he has been an Associate Professor since 2009 and is also with the High-Voltage Research and Tests Laboratory (LINEALT). He has coauthored over 70 papers in international journals and conferences. His research interests include the design of sensors, instrumentation and measurement techniques for high frequency currents, particularly due to partial discharges in noisy environments, and the study and characterization of magneto-optic sensors based on the Faraday Effect for the measurement of currents and the characterization of the behavior of magnetic materials at high frequencies.